Environmental Science and Ecotechnology 29 (2026) 100661

Contents lists available at ScienceDirect

Environmental Science and Ecotechnology

journal homepage: www.journals.elsevier.com/environmental-science-and-ecotechnology/

Original Research

Ephedrine-disrupted synaptogenesis signaling and behavioral abnormalities in adult zebrafish

Yanghui Deng [a,b,c,1], Xingxing Yin [b,1], Changsheng Guo [b], Wenhui Qiu [d], Meng Zhang [b], Xu Tan [b], Jian Xu [a,b,c,*]

[a] College of Water Sciences, Beijing Normal University, Beijing, 100875, China
[b] State Key Laboratory of Environmental Criteria and Risk Assessment, Chinese Research Academy of Environmental Sciences, Beijing, 100012, China
[c] State Environmental Protection Key Laboratory of Ecological Effect and Risk Assessment of Chemicals, Chinese Research Academy of Environmental Sciences, Beijing, 100012, China
[d] Guangdong Provincial Key Laboratory of Soil and Groundwater Pollution Control, School of Environmental Science and Engineering, Southern University of Science and Technology, Shenzhen, 518055, China

ARTICLE INFO

Article history:
Received 28 June 2025
Received in revised form
19 January 2026
Accepted 20 January 2026

Keywords:
Ephedrine
Transcriptomic profiling
Synaptogenesis signaling pathway
Abnormal neurobehavior
Zebrafish

ABSTRACT

Ephedrine is a prevalent sympathomimetic alkaloid and amphetamine-type stimulant precursor that has become a widespread contaminant in global aquatic ecosystems. While the neurotoxic effects of high-dose ephedrine exposure are documented in humans and other mammals, its impact on aquatic vertebrates at environmentally realistic concentrations remains poorly understood. Determining how these persistent residues affect neural development and physiological homeostasis is critical for evaluating ecological risks to aquatic life. Here we show that chronic, low-dose ephedrine exposure impairs neurodevelopment in adult zebrafish by simultaneously disrupting synaptogenesis architecture and neurotransmitter balance. Integrated transcriptomic and histopathological analyses reveal that ephedrine targets the synaptogenesis signaling pathway, resulting in reduced presynaptic vesicles and structural abnormalities in the postsynaptic density. Computational docking and biochemical assays further demonstrate that ephedrine engages the vesicular acetylcholine transporter and tyrosine hydroxylase with high affinity, triggering excitotoxic cascades and biphasic neurochemical dysregulation that manifest as anxiety-like phenotypes and cognitive impairments. These findings indicate that environmentally relevant concentrations of stimulant precursors pose a significant threat to the neural circuit integrity of aquatic species, necessitating urgent regulatory attention to pharmaceutical residues in surface waters.

1. Introduction

Ephedrine is a sympathomimetic alkaloid with both α- and β-adrenergic agonistic activity and has been widely used as a decongestant during surgical anesthesia, as a component in weight-loss products, and as a performance-enhancing substance in sports [1,2]. It is a primary precursor and active metabolite in the synthesis of amphetamine-type stimulants (ATS) [3,4]. In recognition of its potential for diversion and misuse, ephedrine was listed among the first 22 precursor chemicals regulated under the 1988 United Nations Convention against Illicit Traffic in Narcotic Drugs and Psychotropic Substances. According to publicly accessible data from the International Narcotics Control Board, the estimated annual legal demand for ephedrine and its preparations is 20.2 tons in China and as high as 1616 tons in India (https://www.incb.org/incb/index.html). The data compiled by the United Nations Office on Drugs and Crime indicate that approximately 3.3 and 2.6 tons of ephedrine were seized globally in 2019 and 2020, respectively, with China alone reporting seizures totaling 0.5 tons in 2019 [5]. Following therapeutic administration, unmetabolized ephedrine is excreted and discharged into surface waters via municipal sewage systems. In addition, illicit sources contribute to environmental contamination through laboratory effluents,

* Corresponding author. College of Water Sciences, Beijing Normal University, Beijing, 100875, China.
E-mail address: xujian@craes.org.cn (J. Xu).
[1] These two authors contribute equally to this article.

https://doi.org/10.1016/j.ese.2026.100661

improper disposal from clandestine manufacturing, or impurities from the drug trade. Consequently, ephedrine has been frequently detected in aquatic environments, with concentrations in wastewater treatment plant effluents often reaching the μg L^{-1} range [6,7], while levels in surface waters have been reported from ng L^{-1} to μg L^{-1} [8,9]. Prior to 2019, ephedrine concentrations in surface waters in Beijing averaged 22.9 ± 4.9 ng L^{-1} [10]. However, following the COVID-19 pandemic, a substantial increase in environmental ephedrine levels has been documented, with concentrations reaching 86.4 ngL^{-1} in Beijing and a peak of 1000.9 ng L^{-1} observed in the Yangtze River [11,12].

Amphetamine-type stimulants, including ephedrine, have been extensively studied for their potent effects on the central nervous system (CNS), particularly their potential to induce neurotoxicity through interference with neuronal signaling pathways [2,13]. ephedrine, a well-known sympathomimetic agent, has been shown to produce pharmacological effects similar to those of amphetamines [14–16], and high-dose exposure has been linked to neurotoxic outcomes in humans and other mammals, including neurological impairment and abnormal behaviors [14,17,18]. Repeated administration of ephedrine enhances locomotor activity in animal models such as rhesus macaques [17] and rats [19], supporting its effects on dopaminergic (DA) and γ-aminobutyric acid (GABA) neurotransmission. ephedrine has also been reported to stimulate the CNS and increase anxiety-related behaviors in human and rodent studies [13]. In aquatic systems, ephedrine at environmentally relevant concentrations induces developmental neurotoxicity in early-life-stage zebrafish, leading to disrupted spontaneous movement, altered swimming responses, and increased anxiety-like behavior [20]. Furthermore, our previous study confirmed that ephedrine can bioaccumulate in aquatic organisms, highlighting its persistence and potential for long-term effects [21]. These findings suggest that ephedrine residues in surface waters may pose substantial ecological risks, particularly to aquatic vertebrates. However, data on the toxicological effects and underlying mechanisms of ephedrine in aquatic organisms, especially at low and environmentally relevant concentrations, remain limited. Given its structural similarity, functional groups, and pharmacodynamic resemblance to amphetamine and methamphetamine, ephedrine warrants a prioritized evaluation for neurotoxicity in aquatic species. However, the specific neurotoxic responses it elicits at realistic environmental exposures and how these responses relate to behavioral and physiological alterations remain inadequately characterized.

This study aimed to evaluate the neurotoxic effects of environmentally relevant concentrations of ephedrine (0.05–20 μg L^{-1}) in adult zebrafish, with an emphasis on alterations in behavioral phenotypes and neurochemical homeostasis, supported by transcriptomic profiling and quantitative reverse transcription polymerase chain reaction (qRT-PCR) validation. A combination of RNA sequencing, pathway enrichment analysis, and biochemical assays was employed to identify neuronal signaling pathways disrupted by ephedrine exposure. Behavioral endpoints were assessed in parallel with molecular analyses to establish correlations between transcriptional changes and neurobehavioral outcomes, thereby providing an integrated mechanistic understanding of ephedrine-induced neurotoxicity in zebrafish.

2. Materials and methods

2.1. Zebrafish exposure

Sexually mature female zebrafish (*Danio rerio*, AB strain) at 120 days post-fertilization (mean body weight: 400 ± 20 mg) were maintained in a flow-through aquatic housing system (26 ± 0.5 °C; 14:10 light–dark cycle) within a biosecure recirculating aquaculture system. After a 14-day acclimatization in experimental containers, during which no mortality or abnormalities occurred, exposure experiments were conducted in 8 L borosilicate glass tanks containing 5 L of continuously aerated, carbon-filtered municipal water. We randomly allocated fish to four treatment groups using a randomized block design: a negative control (Control) and ephedrine exposures at 0.05 μg L^{-1} (environmentally relevant), 1 μg L^{-1} (peak environmental), and 20 μg L^{-1} (supra-environmental) (n = 105 fish per group). Before exposure, we randomly selected a subset of zebrafish (n = 10; baseline group), euthanized them, and recorded brain weight. The remaining zebrafish were randomly assigned to the Control (n = 10) or ephedrine-exposed (n = 10) groups. Exposures lasted 14 days, and we renewed the water daily to maintain the ephedrine concentrations. After exposure, we measured body weight, length, and brain weight in the exposed zebrafish to calculate the condition factor (K, equation (1)) and brain somatic index (BSI, equation (2)). All procedures adhered to the Organization for Economic Co-operation and Development 305A guidelines to minimize animal use and suffering. The protocols were approved by the Chinese Research Academy of Environmental Sciences Ethics Committee for Scientific and Technological Ethics Review (approval No. CRAES IRB 20250901).

$$K = \frac{W_0}{L_0^3} \times 100\% \quad (1)$$

$$BSI = \frac{W_1}{W_0} \times 100\% \quad (2)$$

In these equations, W_0 represents the total weight of adult zebrafish, W_1 represents the brain weight of adult zebrafish, and L_0 represents the length of adult zebrafish.

2.2. Ephedrine analysis

We quantified ephedrine concentrations in water and zebrafish brain samples using our previously described methodology [22]. Briefly, deuterated internal standards were added to homogenized whole brains. The samples underwent ultrasonic extraction, followed by cleanup using Oasis MCX SPE cartridges (Supplementary Text S1). Daily water samples were filtered through 0.22-μm nylon syringe filters and quantified using Ultra performance liquid chromatography-tandem mass spectrometry (UPLC-MS/MS). We assessed data accuracy by analysing certified reference materials and performing spike-recovery tests (85–115% recovery), and we evaluated method reliability through inter-laboratory comparisons. Supplementary Table S1 reports detailed quality-control results.

2.3. Histopathology analysis

We sampled 15 zebrafish per group 14 days after exposure. Adult brains were dissected, fixed in 10% (w/v) formalin for 24 h, dehydrated, and paraffin-embedded. Serial 4-μm sections were cut using a Leica RM 2016 microtome (Wetzlar, Germany). Sections were hematoxylin–eosin (H&E) stained and examined microscopically (Olympus CX31, Japan) for histopathological alterations.

2.4. Targeted metabolomics

Targeted metabolomics quantified 24 neurochemicals to assess the ephedrine effects on the zebrafish CNS. Epinephrine (EPI), norepinephrine (NE), nicotinic acetylcholine receptors (nAChR),

and serotonin (5-HT) were analyzed by enzyme-linked immunosorbent assay (ELISA), while the remaining 20 neurochemicals were quantified by UPLC-MS/MS using a modified method [23]. The analyte details and MS parameters are presented in Supplementary Table S2.

2.5. RNA isolation, complementary DNA (cDNA) library construction, and sequencing

We euthanized zebrafish ($n = 5$ per group) and dissected brain tissues for RNA sequencing. For each experimental condition, we prepared three biological replicates. Total RNA was extracted and purified using the TRNzol Total RNA Extraction Reagent (Tiangen Biotech Co., Ltd., Beijing, China). We evaluated RNA concentration and purity using a NanoDrop spectrophotometer (Thermo Fisher Scientific, Waltham, MA, USA) and a Qubit fluorometer (Invitrogen, Carlsbad, CA, USA). RNA integrity was assessed with an Agilent 2100 Bioanalyzer (Agilent Technologies, Santa Clara, CA, USA), and only samples that met the quality criteria, including a 28S/18S ratio of 2.0–2.2 and an RNA integrity number value above 9.0, were used for library construction. Library preparation followed standard protocols at the Beijing Genome Institute (BGI, Shenzhen, China), and sequencing was performed on a BGISEQ-500 platform using 50 bp paired-end reads.

2.6. Transcriptomic analysis

We processed raw reads using SOAPnuke v1.4.0 and Trimmomatic v0.36 (parameters: l5 -q0.5 -n0.1; quality control [QC] statistics in Supplementary Table S3). We then mapped clean reads to the zebrafish genome with HISAT v2.1.0 and assembled transcripts using StringTie v1.0.4. Novel genes were predicted using Cuffcompare v0.9-r2. We quantified gene expression with RSEM and identified differential expression (|Fold change [FC]| $\geq$ 1, $p_{adj} \leq 0.01$) using DEGSeq [24] (Supplementary Table S4). For pathway analysis, we used ingenuity pathway analysis (IPA; canonical pathways, diseases/functions, toxicity; Supplementary Table S5) and performed Phyper-based enrichment for Gene Ontology biological process, cellular component, and molecular function terms (GO: BP, CC, MF) and Kyoto Encyclopedia of Genes and Genomes (KEGG) pathways (False discovery rate <0.01).

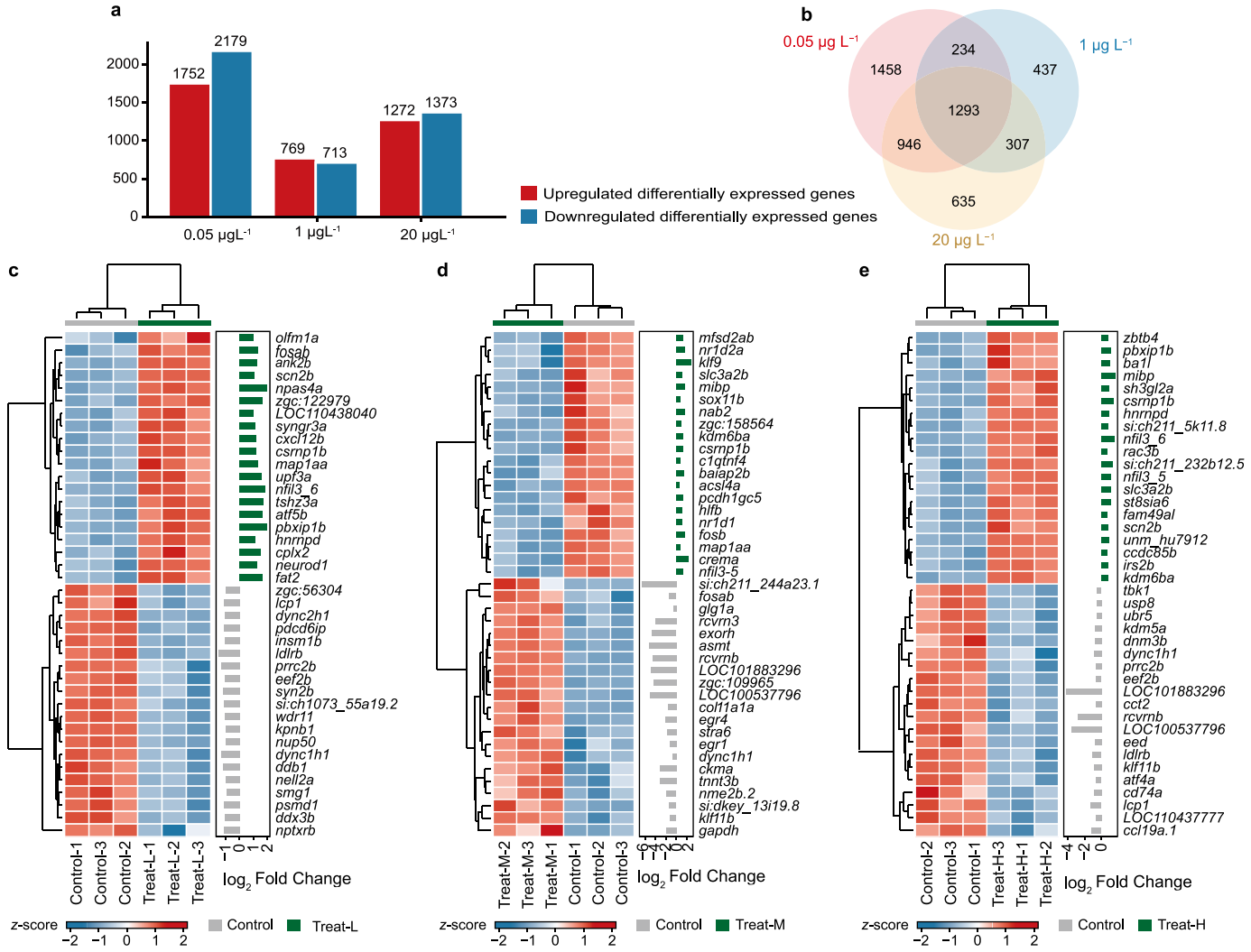

Fig. 1. Differential gene expression across ephedrine exposure concentrations. **a**, Number of differentially expressed genes (DEGs) in zebrafish brain after exposure to 0.05, 1, and 20 μg L^{-1} ephedrine relative to control. **b**, Venn diagram showing the overlap of DEGs among the three ephedrine exposure concentrations. **c**–**e**, Hierarchical clustering of the top 20 upregulated and top 20 downregulated DEGs for 0.05 μg L^{-1} (Treat-L, **c**), 1 μg L^{-1} (Treat-M, **d**), and 20 μg L^{-1} (Treat-H, **e**) ephedrine exposure relative to control. Each group contains three biological replicates, and the number following each group label on the *x*-axis indicates the sample number. In the heat maps, colours indicate significant gene expression changes (*q*-value <0.05) in the treatment groups relative to the control (red, upregulated; blue, downregulated). FC: fold change.

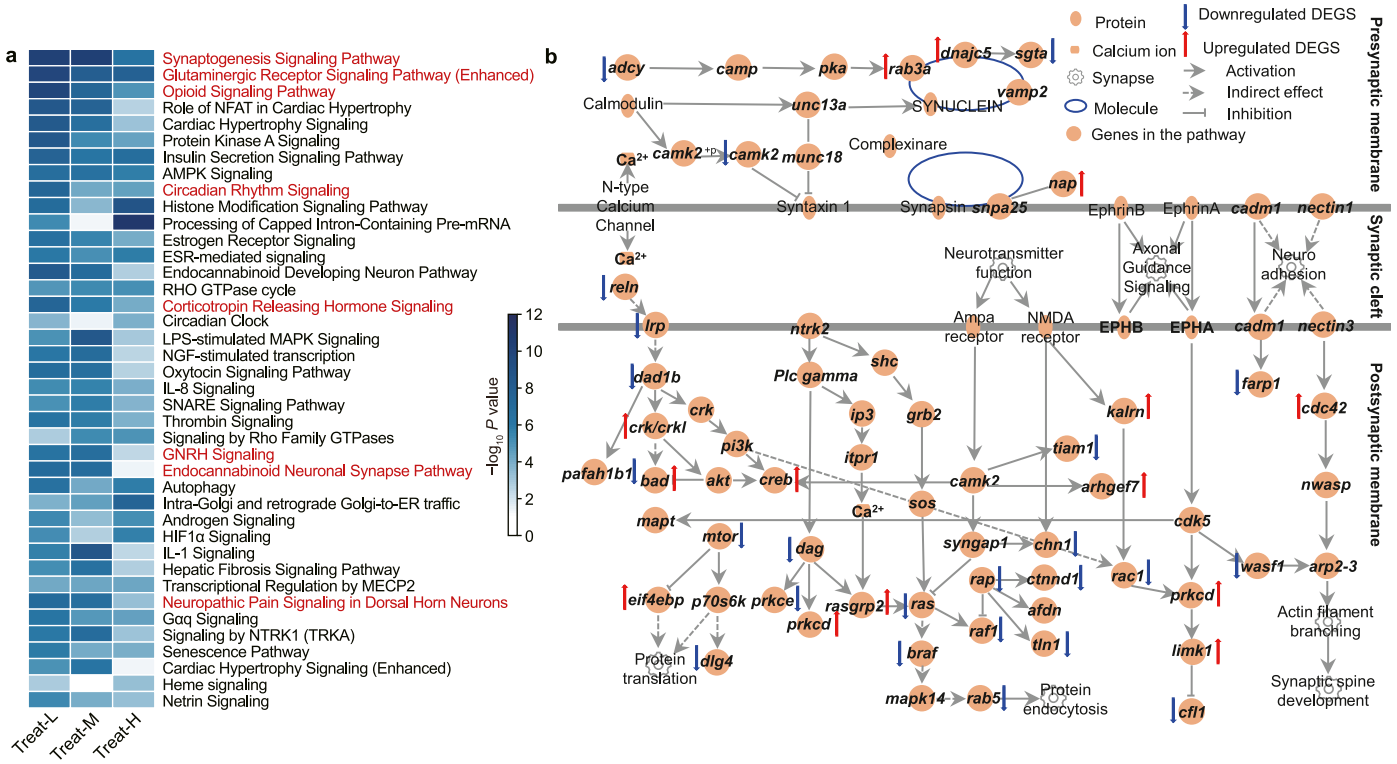
a
Synaptogenesis Signaling Pathway
Glutaminergic Receptor Signaling Pathway (Enhanced)
Opioid Signaling Pathway
Role of NFAT in Cardiac Hypertrophy
Cardiac Hypertrophy Signaling
Protein Kinase A Signaling
Insulin Secretion Signaling Pathway
AMPK Signaling
Circadian Rhythm Signaling
Histone Modification Signaling Pathway
Processing of Capped Intron-Containing Pre-mRNA
Estrogen Receptor Signaling
ESR-mediated signaling
Endocannabinoid Developing Neuron Pathway
RHO GTPase cycle
Corticotropin Releasing Hormone Signaling
Circadian Clock
LPS-stimulated MAPK Signaling
NGF-stimulated transcription
Oxytocin Signaling Pathway
IL-8 Signaling
SNARE Signaling Pathway
Thrombin Signaling
Signaling by Rho Family GTPases
GNRH Signaling
Endocannabinoid Neuronal Synapse Pathway
Autophagy
Intra-Golgi and retrograde Golgi-to-ER traffic
Androgen Signaling
HIF1α Signaling
IL-1 Signaling
Hepatic Fibrosis Signaling Pathway
Transcriptional Regulation by MECP2
Neuropathic Pain Signaling in Dorsal Horn Neurons
Gαq Signaling
Signaling by NTRK1 (TRKA)
Senescence Pathway
Cardiac Hypertrophy Signaling (Enhanced)
Heme signaling
Netrin Signaling
Treat-L
Treat-M
Treat-H
−log10 P value
12
10
8
6
4
2
0
b
Protein
Calcium ion
Synapse
Molecule
Genes in the pathway
Downregulated DEGS
Upregulated DEGS
Activation
Indirect effect
Inhibition
Presynaptic membrane
Synaptic cleft
Postsynaptic membrane
adcy
camp
pka
rab3a
dnajc5
sgta
vamp2
Calmodulin
unc13a
SYNUCLEIN
Ca2+
camk2
camk2
munc18
Complexinare
N-type Calcium Channel
Syntaxin 1
Synapsin
snpa25
nap
EphrinB
EphrinA
cadm1
nectin1
Ca2+
reln
Neurotransmitter function
Axonal Guidance Signaling
Neuro adhesion
lrp
ntrk2
Ampa receptor
NMDA receptor
EPHB
EPHA
cadm1
nectin3
dad1b
Plc gamma
shc
farp1
crk
ip3
grb2
kalrn
cdc42
crk/crkl
pi3k
itpr1
tiam1
pafah1b1
bad
akt
creb
camk2
arhgef7
nwasp
Ca2+
sos
mapt
mtor
cdk5
dag
syngap1
chn1
wasf1
arp2-3
eif4ebp
p70s6k
prkce
rasgrp2
ras
rap
ctnnd1
rac1
prkcd
afdn
Actin filament branching
prkcd
raf1
tln1
limk1
Protein translation
dlg4
braf
Synaptic spine development
mapk14
rab5
Protein endocytosis
cfl1
c
Thermogenesis
Oocyte meiosis
Endocrine resistance
Pathways of neurodegeneration-multiple disease
Amyotrophic lateral sclerosis
Autophagy-animal
Parkinson disease
HIF-1 signaling pathway
Diabetic cardiomyopathy
Protein processing in endoplasmic reticulum
Spinocerebellar ataxia
Human papillomavirus infection
Alzheimer disease
Hepatocellular carcinoma
Shigellosis
Insulin signaling pathway
Huntington disease
Thyroid hormone signaling pathway
MicroRNAs in cancer
Fc epsilon R 1 signaling pathway
Chemical carcinogenesis-reactive oxygen species
Dorso-ventral axis formation
Prion disease
Axon regeneration
Longevity regulating pathway-worm
Yersinia infection
Choline metabolism in cancer
adcy
rab3a
camk2
dnajc5
reln
dlg1
lrp
gsk3
tln1
cif4c
creb
plcg1
sos
arhgef
mapk14
limk1
wasf1
−log10 P value
4
2
Count
10
37
65
93
0.2
0.4
Gene ratio
d
Adrenergic signaling in cardiomyocytes
Human T cell leukemia virus 1 infection
T cell receptor signaling pathway
Neurotrophin signaling pathway
Alzheimer disease
Hepatitis B
Human immunodeficiency virus 1 infection
Oocyte meiosis
Insulin signaling pathway
Pathway of neurodegeneration-multiple disease
Yersinia infection
MicroRNAs in cancer
Chemokine signaling pathway
Fc epsilon R 1 signaling pathway
Growth hormone synthesis, secretion and action
Dopaminergic synapse
HIF-1 signaling pathway
Hedgehog signaling pathway
GnRH signaling pathway
Ras signaling pathway
cAMP signaling pathway
Focal adhesion
Protein processing in endoplasmic reticulum
Shigellosis
Cholesterol metabolism
Longevity regulating pathway-multiple species
dlg
limk1
plcg1
syngap
camk2
sos
dnajc5
mapk14
tln1
lrp
eif4cbp
−log10 P value
2
1
Count
5
18
31
44
0.100
0.125
Gene ratio
e
Vibrio cholerae infection
HIF-1 signaling pathway
Amphetamine addiction
Synaptic vesicle cycle
Protein processing in endoplasmic reticulum
Focal adhesion
Human papillomavirus infection
ECM-receptor interaction
Spinocerebellar ataxia
Hedgehog signaling pathway
Pathways of neurodegeneration-multiple diseases
mTOR signaling pathway
Thyroid hormone signaling pathway
Amyotrophic lateral sclerosis
Autophagy-animal
Insulin signaling pathway
Herpes simplex virus 1 infection
Ferroptosis
Shigellosis
Type II diabetes mellitus
Huntington disease
Notch signaling pathway
AMPK signaling pathway
Adherens junction
Dopaminergic synapse
Phosphatidylinositol signaling system
AGE-RAGE signaling pathway in diabetic complications
Bacterial invasion of epithelial cells
MAPK signaling pathway
Salmonella infection
Axon regeneration
Endocytosis
Phagosome
adcy
camk2
rab3a
dnajc5
dlg1
dag
reln
lrp
plcg1
bad
mapl
tln
gsk3
mtor
ctnndl
creb
plcg1
shc
wasf
sos
ras
mapk14
arhgef
rap
rab5
−log10 P value
7.5
5.0
2.5
Count
9
36
63
90
0.15
0.20
Gene ratio

Fig. 2. Effects of ephedrine exposure on canonical pathways and the synaptogenesis signaling pathway. **a**, Enrichment analysis of the top 40 canonical pathways to 0.05 μg L^{-1} (Treat-L), 1 μg L^{-1} (Treat-M), and 20 μg L^{-1} (Treat-H) ephedrine exposure. Nervous-system-related pathways are labelled in red. **b**, Dysregulation of the synaptogenesis signaling pathway, with blue and red arrows denoting significantly downregulated and upregulated differentially expressed genes (DEGs) after ephedrine exposure, respectively. **c**–**e**, Kyoto Encyclopedia of Genes and Genomes pathway classification and enrichment ratio for genes in the synaptogenesis signaling pathway after exposure to 0.05 μg L^{-1} (**c**), 1 μg L^{-1} (**d**), and 20 μg L^{-1} (**e**) ephedrine.

2.7. Validation of transcriptome analysis using qRT-PCR

We synthesized cDNA using a Quant Script RT Kit (Tiangen Biotech, China). Target genes (Supplementary Table S6) were amplified with Sangon Biotech-synthesized primers. We used β-Actin as the reference gene [25]. qRT-PCR product specificity was confirmed using melting curve analysis. mRNA quantification used efficiency-corrected Ct-based normalization to β-actin [25], with results expressed as $\log_2$ fold change (mean ± standard error of the mean [SEM], $n = 3$). We assessed concordance between RNA-Seq and qRT-PCR using linear regression (OriginPro 8.0) and Pearson correlation analysis (SPSS 18.0).

2.8. Molecular docking

We predicted neurotransmitter-related proteins as potential ephedrine-binding targets, including the type I vesicular glutamate transporter (VGLUT1), tyrosine hydroxylase (TH), glutamate decarboxylase 2 (GAD2), and the vesicular acetylcholine transporter (VACHT). The three-dimensional crystal structures of these proteins were obtained from the Protein Data Bank (PDB; http://www.rcsb.org), and the molecular structure of ephedrine was retrieved from PubChem (https://pubchem.ncbi.nlm.nih.gov). We performed molecular docking simulations by AutoDock Vina (version 1.2.3), with the lowest-binding-energy conformations considered the most probable binding modes [26]. Binding affinities were calculated based on interaction energy scores to assess the likelihood of ephedrine interacting with neuronal protein targets. We visualized the top-scoring conformations, ranked by Vina docking scores (kcal mol^{-1}), in PyMol (version 1.8.x) for structural analysis [27], and characterized the molecular interactions between ephedrine and its putative protein targets using the protein–ligand interaction profiler [28].

2.9. Behavioral assays

We evaluated the neurobehavioral effects of ephedrine exposure using established ethological assays, including open-field exploration, novel tank diving, social preference assessment, and T-maze spatial learning tasks, in adult zebrafish [29]. The experimental groups consisted of 10 individuals per treatment condition ($n = 10$ per group; total $N = 40$), with each fish sequentially assessed across five behavioral paradigms. Specific behavioral testing methods are provided in the Supplementary Text S2. Briefly, all tests were conducted during the light phase in acoustically isolated behavioral chambers maintained under standardized illumination (300 lux), and locomotor activity was recorded using high-resolution digital cameras operating at 60 frames per second. We analyzed behavioral trajectories using EthoVision XT 15.0 (Noldus, the Netherlands), which employs automated video-tracking algorithms to extract kinematic metrics, including swimming velocity, total distance traveled, and spatial occupancy patterns.

2.10. Statistical analysis

We generated figures, including heat maps, in GraphPad Prism 10.0 (GraphPad Software, San Diego, CA, USA) and in R using the pheatmap package. All behavioral, morphometric, somatic index, neurochemical, and gene expression data are presented as mean ± SEM from at least three experimental replicates. We analyzed treatment effects using a one-way analysis of variance with Tukey's post hoc test. Transcriptomic analysis was conducted using DESeq2, and transcripts with $|\log_2 FC| > 1$ and $p < 0.01$ were defined as differentially expressed genes (DEGs). We analyzed qRT-PCR data using the Kruskal–Wallis test with Dunn's multiple comparisons. Statistical significance was denoted as $*p < 0.05$, $**p < 0.01$, $***p < 0.005$, and $****p < 0.001$.

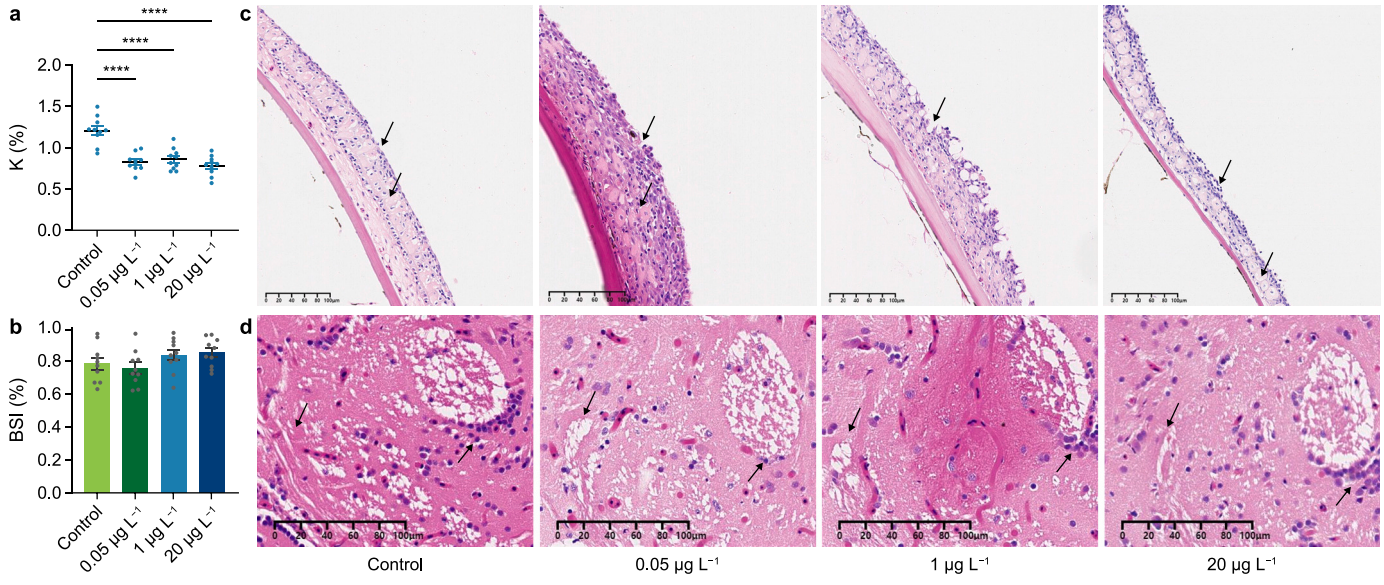

Fig. 3. Condition factor, brain somatic index, and brain histology after ephedrine exposure. **a**, Condition factor (*K*) of zebrafish after 14 days of ephedrine exposure. Asterisks indicate significant differences from control ($****p < 0.001$). **b**, Brain somatic index (*BSI*) after 14 days of ephedrine exposure. **c**,**d**, Representative hematoxylin and eosin-stained sections of the cerebellum (**c**) and midbrain optic tectum (**d**) from zebrafish after 14 days of ephedrine exposure. Arrowheads indicate damaged regions. Scale bars, 100 μm. Data are presented as mean ± standard error of the mean.

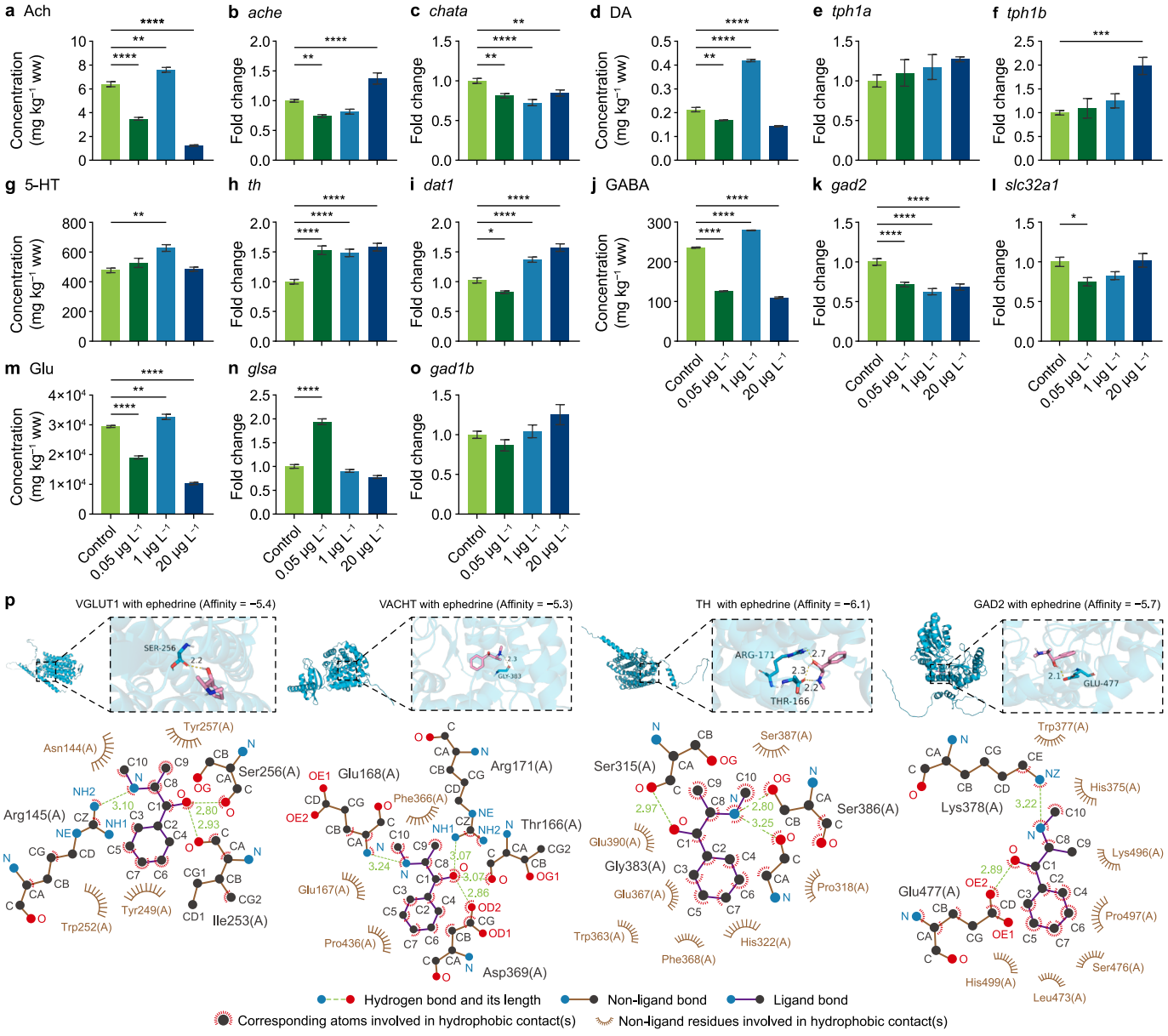

Fig. 4. Neurochemical, gene-expression, and docking analyses after ephedrine exposure. **a**–**o**, Levels of neurochemicals and expression of genes in the major pathways in the zebrafish brain after 14 days of ephedrine exposure ($n = 3$ replicates, 10 zebrafish per replicate). Ach (**a**), *ache* (**b**), *chata* (**c**), DA (**d**), *tph1a* (**e**), *tph1b* (**f**), 5-HT (**g**), *th* (**h**), *dat1* (**i**), GABA (**j**), *gad2* (**k**), *slc32a1* (**l**), Glu (**m**), *glsa* (**n**), and *gad1b* (**o**). Asterisks indicate significant differences from control (*$p < 0.05$, **$p < 0.01$, ***$p < 0.005$, ****$p < 0.001$). **p**, Molecular docking of ephedrine with type I vesicular glutamate transporter (VGLUT1), the vesicular acetylcholine transporter (VACHT), tyrosine hydroxylase (TH), and glutamate decarboxylase 2 (GAD2). Data are presented as mean ± standard error of the mean.

3. Results

3.1. Ephedrine affected the transcriptional profiles of zebrafish brain

No mortality was observed among zebrafish throughout the experimental duration. During the 14-day exposure period, the measured ephedrine concentrations remained within 20% of the nominal values (Supplementary Table S1). ephedrine was not detectable in the brain tissues of either the control or exposed fish at baseline. However, following chronic exposure, ephedrine bioaccumulation in the brain exhibited a dose-dependent pattern, reaching 34.5 ± 11.9, 66.6 ± 12.1, and 489.3 ± 85.8 ng g^{-1} in the respective exposure groups. Transcriptomic profiling revealed 3931 DEGs at 0.05 μg L^{-1} ephedrine (1752 upregulated and 2179 downregulated), 1482 DEGs at 1 μg L^{-1} (769 upregulated and 713 downregulated), and 2645 DEGs at 20 μg L^{-1} (1272 upregulated and 1373 downregulated), with the majority of DEGs exhibiting consistent directional changes across exposure concentrations (Fig. 1). Hierarchical clustering analysis confirmed a uniform dysregulation trend in the gene expression profiles independent of the ephedrine dose. IPA was performed to identify the altered canonical pathways based on DEGs, revealing 40 significantly enriched pathways ($p < 0.01$, $|z\text{-score}| \geq 1$, Fig. 2a), among which 13 were annotated as neurotoxicity related (labelled red in Fig. 2a). Notably, the synaptogenesis signaling pathway emerged as the top-ranked canonical pathway, suggesting that neural disruption represents a primary mode of ephedrine toxicity. Furthermore, the genes involved in the synaptogenesis signaling pathway were significantly affected, even at the lowest tested concentration of

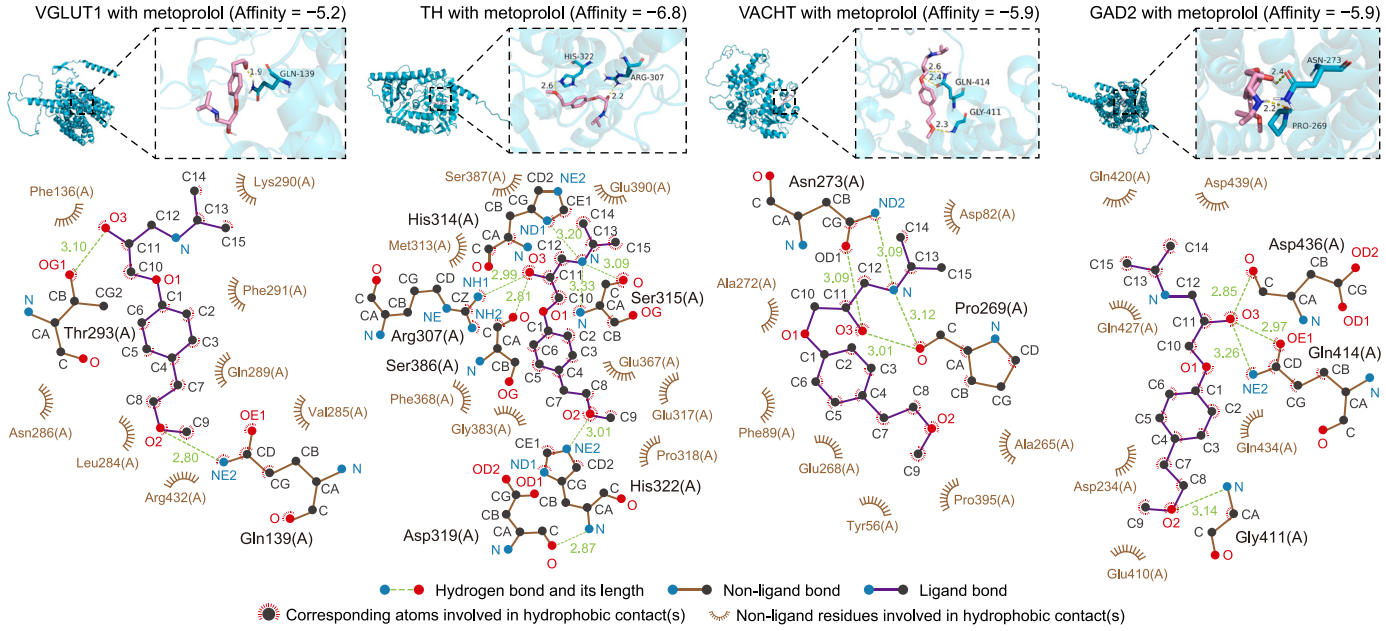

Fig. 5. Molecular docking of metoprolol with type I vesicular glutamate transporter (VGLUT1), the vesicular acetylcholine transporter (VACHT), tyrosine hydroxylase (TH), and glutamate decarboxylase 2 (GAD2).

ephedrine (Fig. 2b). Gene ontology enrichment and the KEGG pathway analyses further indicated that the most enriched molecular functions and signaling cascades were predominantly associated with neurophysiological processes, including neurotrophin signaling, amyotrophic lateral sclerosis, DA and GABAergic synapses, amphetamine addiction, axon guidance, tryptophan and glutathione metabolism, synaptic vesicle cycling, and glutamatergic, cholinergic, and serotonergic synapses (Supplementary Figs. S1–S2). Analysis of the synaptogenesis signaling network in zebrafish (Fig. 2c–e) confirmed that the associated DEGs induced distinct perturbations across multiple nodes, reinforcing the conclusion that ephedrine exerts neurotoxic effects primarily within the CNS.

3.2. Histological characteristics confirmed neuronal damage

Chronic ephedrine exposure induced sublethal physiological alterations, including significant reductions in the condition factor (K; $p < 0.0001$, Fig. 3a and b). Histopathological assessment using H&E staining revealed neurostructural damage in two key brain regions versus the controls: the dorsal telencephalon (hippocampal homologue) and the optic tectum (Fig. 3c and d). The observed pathologies included cytoplasmic vacuolization, neuronal necrosis, and cytotoxic edema with interstitial expansion. Ultrastructural analysis demonstrated synaptic pathology, including presynaptic vesicle depletion and pathological remodeling of the postsynaptic density (PSD), characterized by thinning and fragmentation of this critical synaptic scaffold.

3.3. Ephedrine induced brain neurotransmitter imbalance

Through the comprehensive profiling of 24 neurotransmitters, we identified key disruptions in zebrafish brains (Supplementary Fig. S3). Chronic ephedrine exposure induced concentration-specific alterations across the neurotransmitter pathways. In the cholinergic pathway (Fig. 4a–c), acetylcholine (ACh) levels increased at 1 μg L^{-1} exposure but decreased at 0.05 and 20 μg L^{-1}, while nAChR expression showed 1.4–1.9-fold upregulation. The markers acetylcholinesterase (*ache*) and choline acetyltransferase (*chata*) were downregulated to 0.7–0.8 and 0.7–0.8 of the control levels in the 0.05 and 1 μg L^{-1} groups, respectively. Within the catecholaminergic pathways (Fig. 4d–f), 0.05 μg L^{-1} ephedrine significantly reduced DA (0.8-fold, $p = 0.0011$), precursors tyrosine (0.8-fold, $p < 0.0001$), and levodopa (0.5-fold, $p < 0.0001$), concurrent with the downregulation of the DA transporter (*dat1*, 0.8-fold, $p = 0.0114$), DA receptor (*drd1b*, 1.2-fold), and transcription factor (*nr4a2b*, 0.7-fold, $p = 0.0028$). By contrast, 1 μg L^{-1} exposure elevated DA and precursor levels. NE and EPI increased at 0.05/1 μg L^{-1} (NE: 1.2–1.3-fold; EPI: 1.2–1.5-fold) but decreased at 20 μg L^{-1} (NE: 0.8-fold). TH transcripts increased 1.3–1.4-fold across concentrations, while dopamine β-hydroxylase was specifically activated at 0.05 μg L^{-1} (1.3-fold). For serotonergic signaling (Fig. 4g–i), low-dose ephedrine inhibited tryptophan (0.8-fold, $p = 0.0009$), 5-hydroxytryptophan (0.5-fold, $p < 0.0001$), and 5-hydroxyindoleacetic acid (0.8-fold), whereas intermediate exposure (1 μg L^{-1}) activated these metabolites. Tryptophan hydroxylase genes (*tph1*/*tph2*) exhibited non-significant upregulation. In the glutamate (Glu)/GABAergic axis (Fig. 4j–o), GABA increased exclusively at 1 μg L^{-1} (1.2-fold, $p < 0.0001$) with a concomitant upregulation of synthases (*gad1b*/*gad2*, 1.7-fold), while Glu elevated at 1 μg L^{-1} (1.1-fold, $p = 0.009$). Molecular docking analysis (Fig. 4p) demonstrated a strong binding affinity between ephedrine and the following key neurotransmitter regulators: VGLUT1 (−5.4 kcal mol^{-1}), TH (−6.1 kcal mol^{-1}), GAD2 (−5.7 kcal mol^{-1}), and VACHT (−5.3 kcal mol^{-1}). Molecular docking predicted binding energies below −5.0 kcal mol^{-1} for all ligand–receptor pairs, suggesting a favorable potential interaction between ephedrine and the candidate targets. Comparative docking with metoprolol (Fig. 5), a β-adrenergic antagonist, showed similar affinities: VGLUT1 (−5.2 kcal mol^{-1}), TH (−6.8 kcal mol^{-1}), VACHT (−5.9 kcal mol^{-1}), and GAD2 (−5.9 kcal mol^{-1}). Unlike ephedrine, an adrenergic agonist that drives neurotransmitter release and synaptic excitability, metoprolol acts as an inhibitory antagonist, thereby dampening adrenergic signaling. These opposing pharmacological profiles emphasize that while ephedrine overstimulates multiple

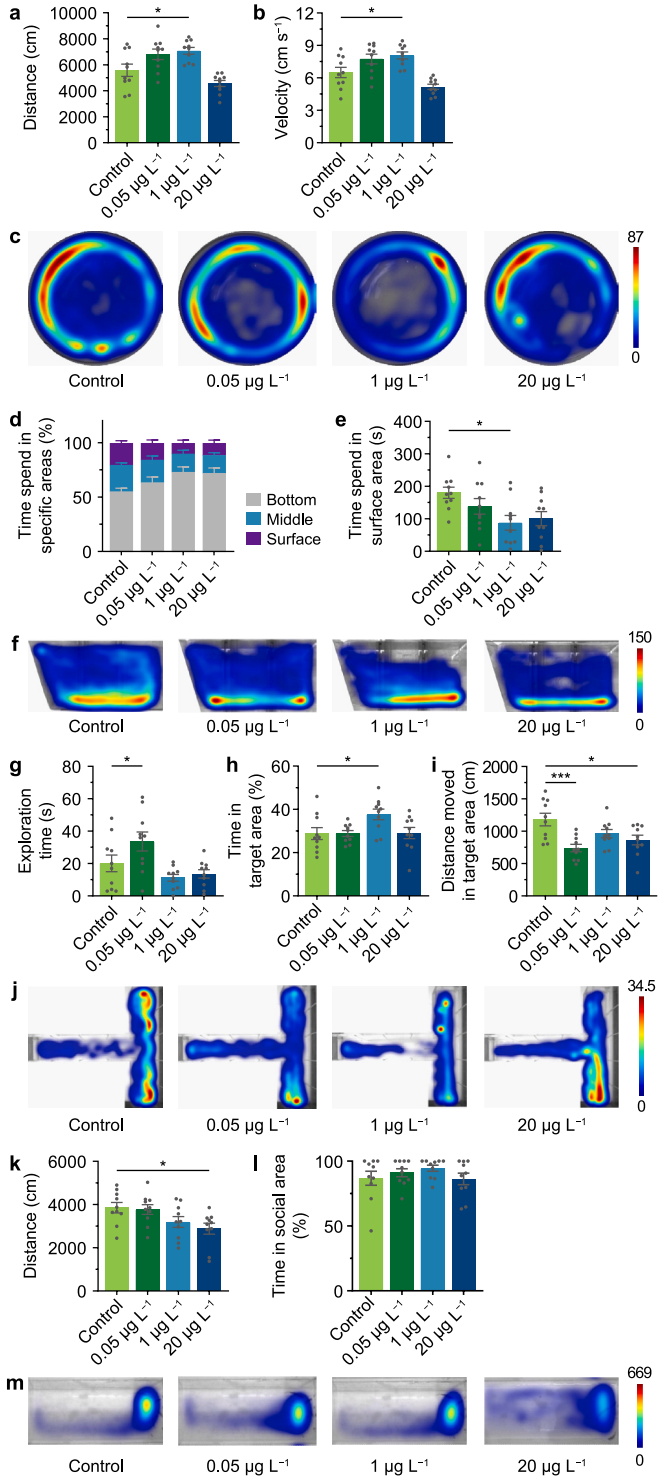

Fig. 6. Behavioural changes in adult zebrafish after ephedrine exposure. **a**–**c**, Open-field test: distance **(a)**, velocity **(b)**, and trajectory heatmap **(c)**. **d**–**f**, Novel-tank test: time spent in specific areas **(d)**, time spent in surface area **(e)**, and trajectory heatmap **(f)**. **g**–**j**, T-maze exploration test: exploration time **(g)**, time in target area **(h)**, distance moved in target area **(i)**, and trajectory heatmap **(j)**, **k**–**m**, Social interaction test: distance **(k)**, time in social area **(l)**, and trajectory heatmap **(m)**. Data are presented as mean ± standard error of the mean; $n = 10$. Asterisks indicate significant differences from control (*$p < 0.05$, ***$p < 0.005$).

neurotransmitter pathways via agonistic mechanisms, metoprolol counteracts by competitively blocking adrenergic signaling, supporting the inference that ephedrine-induced neurotoxicity results from receptor overactivation and synaptic hyperexcitation and may be mitigated by antagonists.

3.4. Ephedrine caused neurobehavioral toxicity

Open-field testing revealed neurobehavioral alterations in zebrafish following ephedrine exposure. Control females exhibited characteristic thigmotaxis with 88.34 ± 2.62% peripheral occupancy, consistent with the established anxiety responses (Fig. 6a and b). While spatial preference remained unaffected, ephedrine induced locomotor hyperactivity at environmental concentrations (0.05–1 μg L^{-1}), evidenced by an increased swimming distance (0.05 μg L^{-1}: 1.2-fold, 1.0 μg L^{-1}: 1.3-fold, $p = 0.0192$), an elevated velocity (0.05 μg L^{-1}: 1.2-fold, 1 μg L^{-1}: 1.2-fold, $p = 0.0182$), and a reduced resting time (0.05 μg L^{-1}: 0.4-fold, $p < 0.0001$, 1 μg L^{-1}: 0.5-fold, $p = 0.0001$), with maximal effects at 0.05 μg L^{-1} (Fig. 6c). New tank testing identified anxiogenic effects at 0.05–1 μg L^{-1}, showing increased bottom-dwelling duration and reduced surface exploration (0.05 μg L^{-1}: 23% decrease; 1 μg L^{-1}: 51% decrease relative to controls; Fig. 6d–f). The T-maze cognitive assessment demonstrated enhanced spatial learning: the 1 μg L^{-1} group reached rewards 44.3% faster than the controls (11.2 ± 2.1 s vs. 20.1 ± 5.1 s). Heatmap analysis indicated expanded exploration of the reward zone in most treatment groups, except at 1 μg L^{-1}, suggesting altered memory consolidation patterns (Fig. 6g–j). Social preference analysis revealed preserved sociability at subtoxic levels; the control zebrafish maintained 75.2 ± 6.8% stimulus-zone occupancy, with significant sociability reduction only at 20 μg L^{-1} (25% decrease, $p = 0.0179$; Fig. 6k–m).

3.5. Ephedrine disrupted the signal transmission between neurons

To delineate the mechanisms underlying ephedrine-induced neurotoxicity, we employed the neuroactive catecholamines EPI and DA as positive controls, both with well-characterized effects on the nervous system. This experimental design capitalizes on the distinct pharmacodynamic profiles of the reference agonists: EPI, a prototypical α/β-adrenoreceptor agonist that elicits sympathetic hyperactivation [30], and DA, the principal regulator of nigrostriatal motor coordination and mesolimbic reward circuitry [31]. The parallel implementation of these controls enables the simultaneous monitoring of two cardinal neurotoxicological endpoints: (i) the autonomic nervous system overdrive via the adrenergic signaling cascades and (ii) DA homeostasis disruption in basal ganglia–thalamocortical loops. Thus, we quantified the main neurotransmitters in the CNS's monoaminergic, cholinergic, GABAergic, and histaminergic systems and performed qRT-PCR analysis of the related genes. Compared with the control group, zebrafish exposed to ephedrine, EPI, and DA exhibited significant alterations in their neurotransmitter and related gene levels (Fig. 7). Exposure to all three compounds resulted in a significant upregulation of the nAChR (1.0–1.9-fold), 5-HT (1.0–1.9-fold), and EPI (1.5–1.8-fold) levels. Conversely, the ACh (0.2–0.9-fold) and Glu (0.01–0.4-fold) levels were significantly downregulated across all exposure groups. However, the DA levels showed compound-specific effects: significant downregulation was observed only in the ephedrine-exposed group, whereas significant upregulation was observed in the DA-exposed (positive control) group. Furthermore, GABA levels were significantly upregulated exclusively in the EPI-exposed group. Strikingly, ephedrine exposure recapitulated the core neurochemical signatures observed in both the EPI- and DA-challenged models, thereby confirming that ephedrine disrupted neuronal signal transmission.

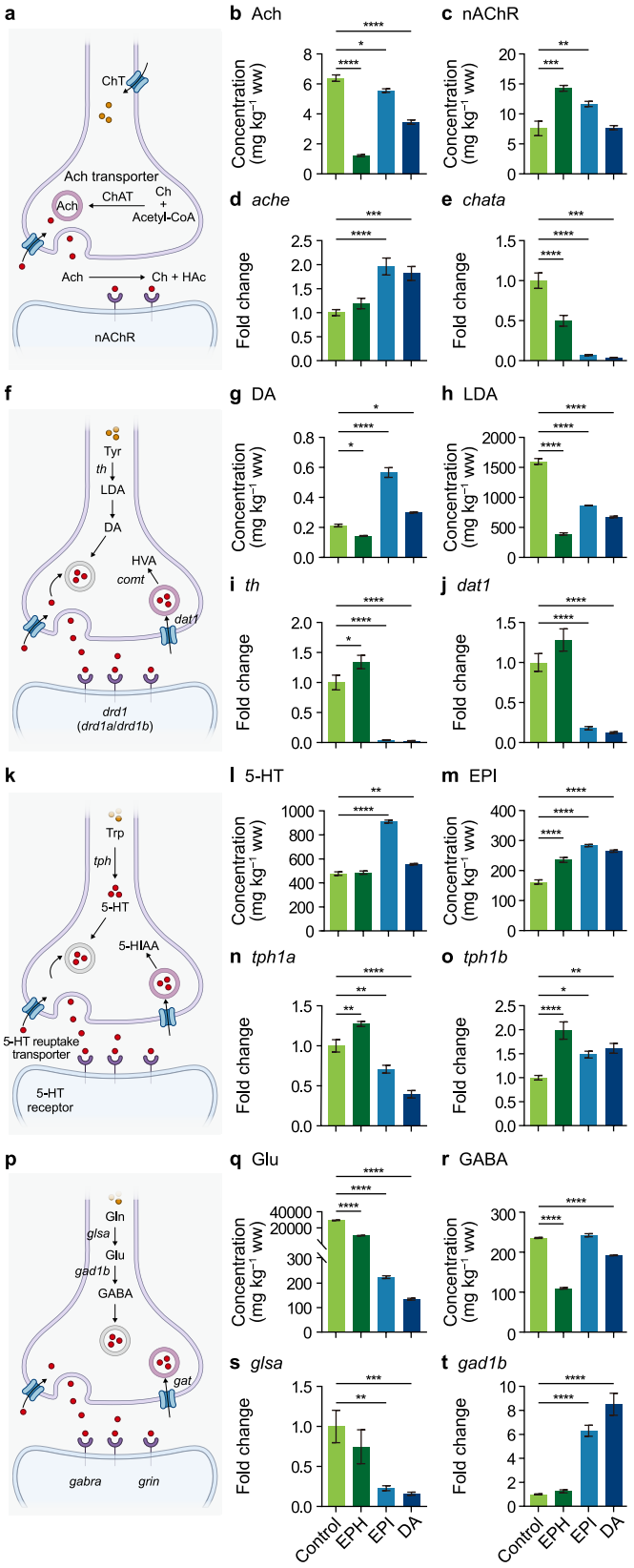

Fig. 7. Neurochemical and gene-expression changes in major pathways of zebrafish brains after 14 days of exposure to ephedrine (20 μg L^{-1}), epinephrine (EPI; 20 μg L^{-1}), and dopamine (DA; 20 μg L^{-1}) (n = 3 replicates, 10 zebrafish per replicate). a, Acetylcholine synthesis, transport, and release in presynaptic neurons. **b–c**, The concentration of Ach (**b**) and nAChR (**c**). **d–e**, Fold change of *ache* (**d**) and *chata* (**e**). **f,** Dopamine synthesis, transport, and release in presynaptic neurons. **g–h**, The concentration of DA (**g**) and LDA (**h**). **i–j,** Fold change of *th* (**i**) and *dat1* (**j**). **k,** 5-Hydroxytryptamine synthesis, transport, and release in presynaptic neurons. **l–m,** The concentration of 5-HT (**l**) and EPI (**m**). **n–o,** Fold change of *tph1a* (**n**) and *thp1b* (**o**). **p,** Glutamic acid synthesis, transport, and release in presynaptic neurons. **q–r,** The concentration of Glu (**q**) and GABA (**r**). **s–t,** Fold change of *glsa* (**s**) and *gad1b* (**t**). Data are presented as mean ± standard error of the mean. Asterisks indicate significant differences from control (*$p < 0.05$, **$p < 0.01$, ***$p < 0.005$, ****$p < 0.001$).

4. Discussion and conclusion

In our previous work, ephedrine emerged as one of the most frequently detected psychoactive contaminants in aquatic systems despite its rapid degradation [32]. ephedrine demonstrated clear bioaccumulation in zebrafish brains, raising concerns that it could compromise aquatic health and destabilize ecosystem function by disrupting neurobehavioral function. Consequently, deciphering ephedrine's neurotoxic mechanisms is critical. Here, using an integrated multi-level approach that combined transcriptomics, histopathology, molecular, and behavioral analyses, we systematically characterized ephedrine-induced neurotoxicity and its interconnections, revealing that even environmentally realistic low concentrations disrupt neural signaling pathways.

Synapses constitute fundamental units for interneuronal communication and mediate complex network functions through chemical/electrical transmission [33,34]. Synaptogenesis, the formation of functional synaptic connections, is critical for nervous system development, plasticity, and cognition. This process occurs from embryonic stages to adulthood under precise genetic, environmental, and activity-dependent regulation. Environmental pollutants have been documented to disrupt zebrafish synaptogenesis, including perfluorononanoic acid [35], propylparaben [36], and neonicotinoid insecticides [37]. In this study, IPA-based canonical pathway analysis identified the synaptogenesis signaling pathway as the most significantly perturbed, indicating impaired synapse formation following ephedrine exposure. More importantly, synaptogenesis signaling involves establishing neurotransmitter release sites in presynaptic neurons [38], in which neurotransmitter identity, concentration dynamics, and degradation critically determine synaptic outcomes. These molecules mediate excitatory/inhibitory effects on target organs [39]. KEGG enrichment analysis of ephedrine-exposed DEGs further revealed significant dysregulation of key neural pathways, including amyotrophic lateral sclerosis, DA, glutamatergic, adrenergic, and cholinergic signaling. Collectively, these findings indicate that ephedrine disrupts both synaptogenesis signaling and neurotransmitter-mediated synaptic transmission, thereby impairing neuronal functions in the zebrafish brain and subsequently affecting synaptic plasticity, learning/memory processes, and brain injury responses.

To validate IPA-predicted dysregulation in synaptogenesis signaling pathways, we conducted systematic histopathological analyses of adult zebrafish brains to determine whether ephedrine exposure induces cellular/tissue-level damage linked to synaptic dysfunction. The significant neuronal pathologies observed in zebrafish following ephedrine exposure, including specific synaptic injuries such as reduced presynaptic vesicle numbers and structural abnormalities in the PSD (e.g., thinning or fragmentation), indicate that ephedrine-mediated disruption of the synaptogenesis signaling pathway in zebrafish may be associated with CNS cytopathy [40]. Moreover, given that synaptic structural integrity is a prerequisite for the precise release and reception of neurotransmitters, we hypothesize that the synthesis, storage, or release of key neurotransmitters (e.g., dopamine and GLU) is impaired, leading to neurochemical imbalances in the CNS [41].

ACh and Ch are essential neurotransmitters in synaptogenesis

and participate in early neural circuit formation [42]. Following ephedrine exposure, significant alterations in ACh levels and its canonical receptor nAChR indicate cholinergic system disruption in zebrafish brains. This conclusion is further supported by the strong binding activity between ephedrine and VACHT (*slc18a3*), a key transporter for efficient neural signal transmission [43]. In addition, activated nAChR can trigger the release of other neurotransmitters [44], explaining the significant upregulation of 5-HT, EPI, and NE post-exposure. NE, DA, and 5-HT serve as critical modulators of neurobehavioral homeostasis, regulating neuronal excitability, synaptic plasticity, and physiological processes, including motor coordination and neuroendocrine functions [45,46]. Notably, the DA levels exhibited biphasic regulation: significant elevation at 1 μg L^{-1} ephedrine but reduction at 0.05 μg L^{-1} and 20 μg L^{-1}. This discordance suggests that ephedrine differentially affects DA and serotonergic synaptic homeostasis by altering the balance between presynaptic synthesis and reuptake. Such neurotransmitter surges likely reflect a compensatory synaptic overdrive that precedes monoaminergic system collapse, analogous to the excitotoxic phases in psychostimulant abuse models [47]. The computational docking of the TH protein with ephedrine (binding energy: −6.1 kcal mol^{-1}) validates this hypothesis. Concurrently, GABA levels and *gad1* expression showed identical trends: significant upregulation at 1 μg L^{-1} ephedrine but downregulation at 0.05 μg L^{-1} and 20 μg L^{-1}, indicating alterations in synaptogenic signaling associated with disruption of the Glu/GABAergic system [48]. Collectively, these findings demonstrate that ephedrine disrupts cholinergic and Glu/GABAergic homeostasis, induces biphasic neurotransmitter dysregulation with presynaptic imbalance, and ultimately perturbs synaptogenesis signaling via excitotoxic mechanisms.

Neurotransmitters play a critical role in regulating a range of neurobehavioral processes, including motor activity, anxiety, depression, learning, and cognition. Previous studies have shown that substances such as methamphetamine and ketamine can disrupt motor behaviors in adult zebrafish [29,49]. One study observed that exposure to ephedrine increased swimming distance and speed in zebrafish larvae, attributed to elevated DA levels and dysregulation of neurodevelopmental genes [20]. Building on these findings, the current study aimed to investigate the effects of ephedrine exposure on zebrafish neurobehaviors, focusing specifically on potential anxiety and depressive-like states. In the novel tank and open-field tests, zebrafish exposed to environmentally relevant concentrations of ephedrine exhibited significant increases in swimming distance and average speed, along with a marked decrease in time spent on the water surface, suggesting a potential elevation in anxiety levels. However, these results were not entirely consistent across the tests. The open-field test, as indicated by the heatmap, revealed a reduction in the time zebrafish spent in the central area of the tank following ephedrine exposure, further supporting the hypothesis that ephedrine exposure increased anxiety. Although anxiety is typically associated with a reduction in 5-HT levels [50], in some instances, elevated 5-HT concentrations can also lead to heightened sympathetic nerve activity, which may contribute to symptoms of anxiety and depression [51]. This dual role of 5-HT is consistent with our findings, in which the observed anxiety-like behaviors in zebrafish following ephedrine exposure may be linked to a significant upregulation of 5-HT levels. Furthermore, the T-maze assessment demonstrated that ephedrine exposure caused significant impairments in zebrafish spatial learning, reinforcing the link between ephedrine-induced neurotoxicity and memory dysfunction. While the social preference test indicated that ephedrine exposure did not alter zebrafish social behavior, the findings from thigmotaxis analyses (open-field and novel tank tests) and cognitive function evaluations suggested a disruption of the zebrafish threat assessment circuitry within the CNS. These multimodal behavioral disruptions, coupled with disturbances in neuroactive substances and histopathological evidence of brain tissue damage, point to a broader mechanism in which ephedrine dysregulates neural signaling pathways in the zebrafish brain.

Altogether, the data delineate a stepwise mechanism in which ephedrine directly binds and inhibits key synaptic proteins (TH, VAChT), downregulates synaptogenesis programs, erodes synaptic ultrastructure (fewer vesicles, abnormal PSD), and disrupts neurotransmitter homeostasis (cholinergic loss, monoaminergic imbalance), ultimately impairing anxiety- and cognition-related circuits and behavior at environmentally relevant concentrations through conserved pathways. A principal limitation is the absence of a monotonic dose–response across endpoints, consistent with nonlinear, potentially hormetic neurotoxicity in which adaptive responses at higher doses can obscure effects evident at low exposures [52–58]. Nevertheless, a low-dose activity within ecologically realistic ranges underscores the need for immediate regulatory scrutiny of ephedrine emissions and heightened vigilance toward structurally related pharmaceuticals, given the risks of food-web bioaccumulation and ecosystem-level impacts.

CRediT authorship contribution statement

Yanghui Deng: Writing - Original Draft, Software, Methodology, Investigation, Formal Analysis, Data Curation. **Xingxing Yin:** Software, Resources, Methodology, Investigation. **Changsheng Guo:** Methodology, Investigation. **Wenhui Qiu:** Writing - Review & Editing, Supervision. **Meng Zhang:** Formal Analysis, Data Curation. **Xu Tan:** Formal Analysis, Data Curation. **Jian Xu:** Writing - Review & Editing, Supervision, Project Administration.

Declaration of competing interest

The authors declare that they have no known competing financial interests or personal relationships that could have appeared to influence the work reported in this paper.

Acknowledgments

This work was funded by the National Science Fund for Distinguished Young Scholars (42325706) and the National Natural Science Foundation of China (42177382, 42307366).

Appendix A. Supplementary data

Supplementary data to this article can be found online at https://doi.org/10.1016/j.ese.2026.100661.

References

[1] N. Oshima, T. Yamashita, S. Hyuga, M. Hyuga, H. Kamakura, M. Yoshimura, T. Maruyama, T. Hakamatsuka, Y. Amakura, T. Hanawa, Y. Goda, Efficiently prepared ephedrine alkaloids-free Ephedra Herb extract: a putative marker and antiproliferative effects, J. Nat. Med. 70 (3) (2016) 554–562.
[2] N. Yang, J. Guo, J. Zhang, S. Gao, Q. Xiang, J. Wen, Y. Huang, C. Rao, Y. Chen, A toxicological review of alkaloids, Drug Chem. Toxicol. 47 (6) (2024) 1267–1281.
[3] D. Gu, C. Guo, S. Hou, J. Lv, Y. Zhang, Q. Feng, Y. Zhang, J. Xu, Kinetic and mechanistic investigation on the decomposition of ketamine by UV-254 nm activated persulfate, Chem. Eng. J. 370 (2019) 19–26.
[4] C. Guo, T. Zhang, S. Hou, J. Lv, Y. Zhang, F. Wu, Z. Hua, W. Meng, H. Zhang, J. Xu, Investigation and application of a new passive sampling technique for in situ monitoring of illicit drugs in waste waters and rivers, Environ. Sci. Technol. 51 (16) (2017) 9101–9108.
[5] The United Nations Office on Drugs and Crime, UNODC, Word Drug Report 2022, 2022.
[6] D.R. Baker, V. Ocenaskova, M. Kvicalova, B. Kasprzyk-Hordern, Drugs of abuse

in wastewater and suspended particulate matter–further developments in sewage epidemiology, Environ. Int. 48 (2012) 28–38.
[7] K. Watanabe, C.M. Batikian, D. Pelley, B. Carlson, J. Pitt, R.M. Gersberg, Occurrence of stimulant drugs of abuse in a San Diego, CA, stream and their consumption rates in the neighboring community, Water, Air, Soil Pollut. 231 (5) (2020) 202.
[8] A. Mendoza, B. Zonja, N. Mastroianni, N. Negreira, M. Lopez de Alda, S. Perez, D. Barcelo, A. Gil, Y. Valcarcel, Drugs of abuse, cytostatic drugs and iodinated contrast media in tap water from the Madrid region (central Spain): a case study to analyse their occurrence and human health risk characterization, Environ. Int. 86 (2016) 107–118.
[9] W. Wang, C. Guo, L. Chen, Z. Qiu, X. Yin, J. Xu, Simultaneous enantioselective analysis of illicit drugs in wastewater and surface water by chiral LC–MS/MS: a pilot study on a wastewater treatment plant and its receiving river, Environ. Pollut. (2021) 116424.
[10] Y. Zhang, T. Zhang, C. Guo, J. Lv, Z. Hua, S. Hou, Y. Zhang, W. Meng, J. Xu, Drugs of abuse and their metabolites in the urban rivers of Beijing, China: occurrence, distribution, and potential environmental risk, Sci. Total Environ. 579 (2017) 305–313.
[11] H. Huang, Y. Bai, Y. Zhang, J. Huang, J. Qin, X. Li, Occurrence and transformation of Ephedrine/Pseudoephedrine and methcathinone in wastewater in China, Environ. Sci. Technol. 56 (14) (2022) 10249–10257.
[12] J. Zhao, C. Guo, Q. Yang, W. Liu, H. Zhang, Y. Luo, Y. Zhang, L. Wang, C. Chen, J. Xu, Comprehensive monitoring and prioritizing for contaminants of emerging concern in the Upper Yangtze River, China: an integrated approach, J. Hazard. Mater. 480 (5) (2024) 135835.
[13] L.D. Chait, Factors influencing the reinforcing and subjective effects of ephedrine in humans, Psychopharmacology 113 (3–4) (1994) 381–387.
[14] R. Guo, G. Liu, M. Du, Y. Shi, P. Jiang, X. Liu, L. Liu, J. Liu, Y. Xu, Early ketamine exposure results in cardiac enlargement and heart dysfunction in Xenopus embryos, BMC Anesthesiol. 16 (2016) 16–23.
[15] M. Parolini, S. Magni, S. Castiglioni, E. Zuccato, A. Binelli, Realistic mixture of illicit drugs impaired the oxidative status of the zebra mussel (Dreissena polymorpha), Chemosphere 128 (2015) 96–102.
[16] Z. Wang, Z. Xu, X. Li, Impacts of methamphetamine and ketamine on C.elegans's physiological functions at environmentally relevant concentrations and eco-risk assessment in surface waters, J. Hazard. Mater. 363 (2019) 268–276.
[17] Z. Sun, Y. Ma, S. Duan, L. Xie, J. Lv, J. Huang, Z. Lin, R. Guo, S. Ma, cAMP response element binding protein expression in the hippocampus of rhesus macaques with chronic ephedrine addiction, BioMed Res. Int. 2017 (2017) 1–8.
[18] G. de Guglielmo, A. Iemolo, A. Nur, A. Turner, P. Montilla-Perez, A. Martinez, C. Crook, A. Roberts, F. Telese, Reelin deficiency exacerbates cocaine-induced hyperlocomotion by enhancing neuronal activity in the dorsomedial striatum, Gene Brain Behav. 21 (7) (2022).
[19] D.K. Miller, J.R. Nation, P.J. Wellman, Sensitization of anorexia and locomotion induced by chronic administration of ephedrine in rats, Life Sci. 65 (5) (1999) 501–511.
[20] D.-D. Ma, W.-J. Shi, S.-Y. Li, J.-G. Zhang, Z.-J. Lu, X.-B. Long, X. Liu, C.-S. Huang, G.-G. Ying, Ephedrine and cocaine cause developmental neurotoxicity and abnormal behavior in zebrafish, Aquat. Toxicol. 265 (2023) 106765.
[21] X. Yin, C. Guo, Y. Deng, Z. Qin, Y. Zhang, Y. Teng, J. Xu, Organ-Specific accumulation and toxicokinetics of ephedrine in adult zebrafish (*Danio rerio*), Environ. Sci. 42 (3) (2021) 1496–1502.
[22] X. Yin, C. Guo, Y. Deng, X. Jin, Y. Teng, J. Xu, F. Wu, Tissue-specific accumulation, elimination, and toxicokinetic of illicit drugs in adult zebrafish (*Danio rerio*), Sci. Total Environ. 792 (2021) 148153.
[23] S. Liu, J. Dong, X. Fang, X. Yan, H. Zhang, Y. Hu, Q. Zhu, R. Li, Q. Liu, S. Liu, C. Liao, G. Jiang, Nanoscale zinc-based metal–organic frameworks induce neurotoxicity by disturbing the metabolism of catecholamine neurotransmitters, Environ. Sci. Technol. 57 (13) (2023) 5380–5390.
[24] L. Wang, Z. Feng, X. Wang, X. Wang, X. Zhang, DEGseq: an R package for identifying differentially expressed genes from RNA-seq data, Bioinformatics 26 (1) (2010) 136–138.
[25] K.J. Livak, T.D. Schmittgen, Analysis of relative gene expression data using real-time quantitative PCR and the $2-\Delta\Delta CT$ method, Methods 25 (4) (2001) 402–408.
[26] G.M. Morris, R. Huey, W. Lindstrom, M.F. Sanner, R.K. Belew, D.S. Goodsell, A.J. Olson, AutoDock4 and AutoDockTools4: automated docking with selective receptor flexibility, J. Comput. Chem. 30 (16) (2009) 2785–2791.
[27] S. Yuan, H.C.S. Chan, Z. Hu, Using PyMOL as a platform for computational drug design, Wires Comput Mol Sci. 7 (2) (2017).
[28] M.F. Adasme, K.L. Linnemann, S.N. Bolz, F. Kaiser, S. Salentin, V.J. Haupt, M. Schroeder, Plip 2021: expanding the scope of the protein–ligand interaction profiler to DNA and RNA, Nucleic Acids Res. 49 (W1) (2021) W530–W534.
[29] X. Yin, Y. Deng, C. Guo, C. Ding, J. Xu, F. Wu, Behavioral changes and metabolic responses of adult zebrafish (*Danio Rerio*) exposed to methamphetamine, ACS ES&T Water 3 (8) (2023) 2551–2559.
[30] A. William Tank, D.L. W, Peripheral and central effects of circulating catecholamines, Compr. Physiol. 5 (1) (2015) 1–15.
[31] K.M.C.G. Schoenbaum, Dopamine, Curr. Biol. 32 (2022) R817–R824, 2022.
[32] Y. Zhang, C. Guo, R. Wu, S. Hou, Y. Liu, J. Zhao, M. Jiang, J. Xu, F. Wu, Global occurrence, distribution, and ecological risk assessment of psychopharmaceuticals and illicit drugs in surface water environment: a meta-analysis, Water Res. 263 (2024).
[33] C.C. Garner, R.G. Zhai, E.D. Gundelfinger, N.E. Ziv, Molecular mechanisms of CNS synaptogenesis, Trends Neurosci. 25 (5) (2002) 243–250.
[34] J.-P. Bourgeois, P.S. Goldman-Rakic, P. Rakic, Synaptogenesis in the prefrontal cortex of rhesus monkeys, Cerebr. Cortex 4 (1) (1994) 78–96.
[35] S. Liu, W. Qiu, R. Li, B. Chen, X. Wu, J.T. Magnuson, B. Xu, S. Luo, E.G. Xu, C. Zheng, Perfluorononanoic acid induces neurotoxicity via synaptogenesis signaling in zebrafish, Environ. Sci. Technol. 57 (9) (2023) 3783–3793.
[36] C. Merola, G. Caioni, C. Bertolucci, T. Lucon-Xiccato, B.B. Savaşçı, S. Tait, M. Casella, S. Camerini, E. Benedetti, M. Perugini, Embryonic and larval exposure to propylparaben induces developmental and long-term neurotoxicity in zebrafish model, Sci. Total Environ. 912 (2024).
[37] S. Könemann, M. von Wyl, C. vom Berg, Zebrafish Larvae rapidly recover from Locomotor effects and neuromuscular alterations induced by cholinergic insecticides, Environ. Sci. Technol. 56 (12) (2022) 8449–8462.
[38] S. Lewis, Signalling synaptogenesis, Nat. Rev. Neurosci. 17 (11) (2016), 670-670.
[39] J. Liang, Z. Yang, C. Zhou, Excitation-Inhibition balance, neural criticality, and activities in neuronal circuits, Neuroscientist 31 (1) (2025) 31–46.
[40] D.M. Wilson, M.R. Cookson, L. Van Den Bosch, H. Zetterberg, D.M. Holtzman, I. Dewachter, Hallmarks of neurodegenerative diseases, Cell 186 (4) (2023) 693–714.
[41] X. Li, L. Qin, Y. Li, H. Yu, Z. Zhang, C. Tao, Y. Liu, Y. Xue, X. Zhang, Z. Xu, Y. Wang, H. Lou, Z. Tan, P. Saftig, Z. Chen, T. Xu, G. Bi, S. Duan, Z. Gao, Presynaptic endosomal cathepsin D regulates the biogenesis of GABAergic synaptic vesicles, Cell Rep. 28 (4) (2019) 1015–1028.
[42] X. Wang, D. Zhang, W. Song, C. Cai, Z. Zhou, Q. Fu, X. Yan, Y. Cao, M. Fang, Neuroprotective effects of the aerial parts of Polygala tenuifolia Willd extract on scopolamine-induced learning and memory impairments in mice, Biomedical Reports 13 (5) (2020) 37.
[43] N.E. Loureiro-dos-Santos, M.A.M. Prado, R.A.D. Reis, P.F. Gardino, M.C. de Mello, F.G. de Mello, Regulation of vesicular acetylcholine transporter by the activation of excitatory amino acid receptors in the avian retina, Cell. Mol. Neurobiol. 22 (5–6) (2002) 727–740.
[44] Marina R. Picciotto, Michael J. Higley, Yann S. Mineur, Acetylcholine as a neuromodulator: Cholinergic signaling shapes nervous System function and behavior, Neuron 76 (1) (2012) 116–129.
[45] J. Haller, G.B. Makara, M.R. Kruk, Catecholaminergic involvement in the control of aggression: hormones, the peripheral sympathetic, and central noradrenergic systems, Neurosci. Biobehav. Rev. 22 (1) (1997) 85–97.
[46] A. Pertovaara, Noradrenergic pain modulation, Prog. Neurobiol. 80 (2) (2006) 53–83.
[47] P.H. Chipman, R.D. Fetter, L.C. Panzera, S.J. Bergerson, D. Karmelic, S. Yokoyama, M.B. Hoppa, G.W. Davis, NMDAR-dependent presynaptic homeostasis in adult hippocampus: synapse growth and cross-modal inhibitory plasticity, Neuron 110 (20) (2022) 3302–3317.
[48] K. Horzmann, J. Freeman, Zebrafish get connected: investigating neurotransmission targets and alterations in chemical toxicity, Toxics 4 (19) (2016).
[49] P. Michelotti, V.A. Quadros, M.E. Pereira, D.B. Rosemberg, Ketamine modulates aggressive behavior in adult zebrafish, Neurosci. Lett. 684 (2018) 164–168.
[50] N. Deo, G. Redpath, Serotonin receptor and transporter endocytosis is an important factor in the cellular basis of depression and anxiety, Front. Cell. Neurosci. 15 (2022).
[51] F.G. Graeff, F.S. Guimaraes, T. DeAndrade, J.F.W. Deakin, Role of 5-HT in stress, anxiety, and depression, Pharmacol., Biochem. Behav. 54 (1) (1996) 129–141.
[52] J.P. Myers, R.T. Zoeller, W.V. Welshons, F.S. vom Saal, A.M. Soto, T. Shioda, D.-H. Lee, D.R. Jacobs, J.J. Heindel, T.B. Hayes, T. Colborn, L.N. Vandenberg, Hormones and endocrine-disrupting chemicals: Low-Dose effects and nonmonotonic dose responses, Endocr. Rev. 33 (3) (2012) 378–455.
[53] M.C. Rillig, A. Lehmann, M. Bi, Hormesis as a hidden hand in global environmental change? Environ. Sci. Technol. 59 (6) (2025) 2887–2890.
[54] Y. Yang, C.T. Leung, J. Yang, Q. Wang, Y. Shao, B. Kang, A.S.-T. Wong, R.S.S. Wu, K.P. Lai, Epigenetic responses induced by transgenerational and multigenerational exposure alter the plasticity of fish to neurotoxic effects of triclosan, Environ. Sci. Technol. 404 (1) (2025) 77–87.
[55] Y. Cui, J. Gao, M. Zhao, Y. Guo, Y. Zhao, Z. Wang, Deciphering the interaction impacts between antiseptic benzethonium chloride and biofilm nitrification system: performance, resistance mechanisms and biodegradation, Water Res. 240 (2023) 120062.
[56] X. Liu, Q. Lu, M. Du, Q. Xu, D. Wang, Hormesis-Like effects of Tetrabromobisphenol A on anaerobic digestion: responses of metabolic activity and microbial community, Environ. Sci. Technol. 56 (16) (2022) 11277–11287.
[57] F. Ullah, H. Gul, N. Desneux, X. Gao, D. Song, Imidacloprid-induced hormesis effects on demographic traits of the melon aphid, Aphis gossypii, Entomol. Gen. 39 (3–4) (2019) 325–337.
[58] T. Sun, C. Ji, F. Li, H. Wu, Time is ripe for targeting Per- and Polyfluoroalkyl substances-induced hormesis: global aquatic hotspots and implications for ecological risk assessment, Environ. Sci. Technol. 58 (21) (2024) 9314–9327.